



## Research Note

# Hydrogen and oxygen adsorption stoichiometries on silica supported ruthenium nanoparticles

Romain Berthoud<sup>a</sup>, Pierre Délichère<sup>b</sup>, David Gajan<sup>a</sup>, Wayne Lukens<sup>c</sup>, Katrin Pelzer<sup>d</sup>, Jean-Marie Basset<sup>a</sup>, Jean-Pierre Candy<sup>a,\*</sup>, Christophe Copéret<sup>a,\*</sup>

<sup>a</sup> Laboratoire de Chimie, Catalyse, Polymères et Procédés, ESCPE-Lyon, 43, Bd. du 11 Novembre, F-69616 Villeurbanne, France

<sup>b</sup> Institut de Recherches sur la Catalyse et l'Environnement de Lyon (IRCELYON, CNRS), Université de Lyon, 2, Avenue Albert Einstein, 69626 Villeurbanne Cedex, France

<sup>c</sup> Chemical Sciences Division Lawrence Berkeley National Laboratory, Berkeley, CA 94720, USA

<sup>d</sup> Department for Inorganic Chemistry, Fritz-Haber-Institute of the Max-Planck-Society, Faradayweg 4-6, 14195 Berlin, Germany

## ARTICLE INFO

## Article history:

Received 11 August 2008  
Revised 30 September 2008  
Accepted 5 October 2008  
Available online 8 November 2008

## Keywords:

Ruthenium  
Particles  
Silica  
H<sub>2</sub>  
O<sub>2</sub>  
Adsorption

## ABSTRACT

Treatment under H<sub>2</sub> at 300 °C of Ru(COD)(COT) dispersed on silica yields 2 nm ruthenium nanoparticles, [Ru<sub>p</sub>/SiO<sub>2</sub>], according to EXAFS, HRTEM and XPS. H<sub>2</sub> adsorption measurements on [Ru<sub>p</sub>/SiO<sub>2</sub>] in the absence of O<sub>2</sub> show that Ru particles adsorb up to ca. 2H per surface ruthenium atoms (2H/Ru<sub>s</sub>) on various samples; this technique can therefore be used to measure the dispersion of Ru particles. In contrast, O<sub>2</sub> adsorption on [Ru<sub>p</sub>/SiO<sub>2</sub>] leads to a partial oxidation of the bulk at 25 °C, to RuO<sub>2</sub> at 200 °C and to sintering upon further reduction under H<sub>2</sub>, showing that O<sub>2</sub> adsorption cannot be used to measure the dispersion of Ru particles.

© 2008 Published by Elsevier Inc.

## 1. Introduction

Supported metal nanoparticles constitutes a large class of heterogeneous catalysts [1], and their properties (activity, selectivity) are often, if not always, associated to their size and shape [2]. Thus, a precise measurement of their size, often referred to as dispersion, is critical if one wants to understand their reactivity and try to develop structure–reactivity relationships. Of various methods targeted at measuring particles dispersion measurements, H<sub>2</sub> and O<sub>2</sub> adsorptions [3] are very useful and convenient: however this approach relies on the knowledge of the number of hydrogen adsorbed per surface atoms, and this stoichiometric ratio depends on the metals. In the case of silica-supported particles of platinum [4,5] and rhodium [6], extended studies on adsorption measurements, based on Langmuir adsorption isotherms, correlated to particle size distributions (determined by transmission electron microscopy), led to the stoichiometry of 2H/M<sub>s</sub>, in contrast to the former accepted value of 1H/M<sub>s</sub> [7,8]. In the case of ruthenium, early studies on Ru powders suggested a ratio of 1.5 by comparing H<sub>2</sub> and N<sub>2</sub> adsorptions [9]. Later studies on powder and supported samples [10,11] were consistent with a stoichiometry of 1H<sub>irrev</sub>/Ru<sub>s</sub> (or slightly higher), which was not size dependant, while others claimed a value of 2 H/Ru<sub>s</sub> [12]. It was also proposed

using solid-state NMR that hydrogen chemisorption greatly underestimated the ruthenium dispersion [13]. Thus, it appears that no real consensus has been reached for the H/Ru<sub>s</sub> stoichiometry and for the method to perform chemisorption measurements. In the case of O<sub>2</sub>, various studies on ruthenium diverged in the O/Ru<sub>s</sub> stoichiometry, ranging from 1 to 2 [11,14], but agreed on its high dependence toward the method of preparation and the size of the particles.

Here, by using EXAFS, HRTEM and XPS in combination with H<sub>2</sub> adsorption measurements, we show that fully reduced Ru<sub>p</sub> supported on silica, [Ru<sub>p</sub>/SiO<sub>2</sub>], (reproducibly and reversibly) adsorb 2H/Ru<sub>s</sub>.<sup>1</sup> We also show that adsorption of O<sub>2</sub> leads to partial oxidation of the bulk at 25 °C. Finally, while oxidation/reduction cycles do not significantly affect the O adsorption on Ru<sub>t</sub>, we show that the H<sub>2</sub> adsorption varies, which is consistent with a modification of the adsorption properties of Ru particles, most likely related to the sintering of the particles after each cycle.

## 2. Experimental

### 2.1. Materials

All experiments were carried out under dry and oxygen free Ar using either standard Schlenk or glove-box techniques for

\* Corresponding authors. Fax: +33 472431795.

E-mail addresses: candy@cpe.fr (J.-P. Candy), coperet@cpe.fr (C. Copéret).

<sup>1</sup> This stoichiometry of 2H/Ru<sub>s</sub> is likely specific of silica supported Ru particles.

organometallic synthesis. For the syntheses and the treatments of the surface species, reactions were carried out using high vacuum lines ( $10^{-5}$  mbar) and glove-box techniques.  $H_2$  (reactants and adsorbates) was purified over R3-11 BASF catalyst/MS 4 Å prior to use.  $O_2$  was dried over MS 4 Å prior to use. Pentane was distilled from NaK under  $N_2$ . Elemental analyses were performed at the CNRS Central Analysis Department of Solaize (Ru) and at the University of Bourgogne, Dijon (C and H).

Two types of catalysts were prepared for adsorption measurements, namely  $[Ru_p/SiO_2]$  and  $[Ru_p/SBA-15]$ . Silica (Aerosil Degussa,  $200\text{ m}^2\text{ g}^{-1}$ ) was compacted with distilled water, calcined at  $500^\circ\text{C}$  under air for 2 h and treated under vacuum ( $10^{-5}$  mbar) at  $500^\circ\text{C}$  for 12 h and then at  $700^\circ\text{C}$  for 4 h (support referred to as  $SiO_{2-(700)}$ ). SBA-15, a mesoporous silica, was prepared from  $Si(OEt)_4$  according to literature conditions [15]. After calcination at  $500^\circ\text{C}$  under air for 5 h and then treatment under vacuum at  $500^\circ\text{C}$  for 15 h, SBA-15<sub>(500)</sub> was obtained with the following characteristic: surface area =  $760\text{ m}^2\text{ g}^{-1}$  and average pore diameter = 7 nm. The supported Ru particles were prepared by adapting a literature procedure [16] as follows: typically,  $Ru(1,5\text{-cyclooctadiene})(1,3,5\text{-cyclooctatriene})$  [17] and  $SiO_{2-(700)}$  (or SBA-15<sub>(500)</sub>) were loaded in a 370-mL reactor, and ca. 3 mL of pentane were added. This mixture was stirred to insure a homogeneous dispersion of the complex on the support. The solvent was evaporated to dryness, and this procedure was repeated twice. The solid was finally dried under vacuum ( $10^{-5}$  mbar) for 1 h, yielding a yellow powder. Then, this solid was loaded in a 470 mL reactor flask at  $25^\circ\text{C}$ ,  $H_2$  (666 mbar) was added, and the reactor was heated at  $300^\circ\text{C}$  for 24 h. After evacuation of the gas phase at  $25^\circ\text{C}$ , a second  $H_2$  treatment under the same reaction conditions was performed. Finally, the reactor is evacuated under vacuum ( $10^{-5}$  mbar) for 30 min, yielding  $Ru_p/SiO_2$ , 0.65 wt% Ru (or  $Ru_p/SBA-15$ , 1.92 wt% Ru). For all the samples prepared, no carbon is detected by elemental analysis ( $<0.1$  wt%).

## 2.2. XPS

X-ray photoelectron spectroscopy was performed in a Kratos Axis Ultra DLD spectrometer, using a monochromated  $AlK\alpha$  X-ray with a pass energy of 20 eV and a coaxial charge neutralizer. The base pressure in the analysis chamber was better than  $5 \times 10^{-8}$  Pa. The samples were prepared in a glove-box on an Indium foil sample holder and transferred into the spectrometer under inert atmosphere.

XPS spectra of Ru3d, C1s, Si2p and O1s levels were measured at a normal angle with respect to the plane of the surface. High-resolution spectra were corrected for charging effects by assigning a value of 284.6 eV to the C1s peak (adventitious carbon). Binding energies were determined with an accuracy of  $\pm 0.2$  eV. Synthetic components on Ru3d–C1s were analyzed with a Shirley background subtraction and a peak shape with a combination of Gaussian and Lorentzian (30% Lorentzian).

## 2.3. Determination of particle size by TEM

All samples for TEM analysis were prepared from powder samples by dry preparation in a glove box and were transferred inside a special vacuum transfer holder under inert atmosphere to a Philips CM200 transmission electron microscope. The acceleration voltage was 200 kV.

## 2.4. Determination of particle size by EXAFS

Transmission data were obtained at Stanford Synchrotron Radiation Laboratory on beam-line 11-2. The data reduction was performed by standard procedures using the programs EXAFSPAK and

Athena [18,19]. The background was removed by fitting a polynomial to the pre-edge of the data such that the post-edge spectrum followed the Victoreen function  $\mu_{vic}$ . The reduced sample was loaded in the glove-box in a cell tightly closed with aluminized mylar windows.

Fitting of the spectrum was done on the  $k^3$  weighted data using Artemis/Ifeffit [19,20]. The program FEFF7 was used to calculate theoretical values for  $S_i$ ,  $F_i$ ,  $\lambda_i$ ,  $\phi_i$ , and  $\phi_c$  [21]. The  $\Delta E_0$  parameter was allowed to vary during fitting of the EXAFS spectra; for a given fit,  $\Delta E_0$  was constrained to be the same for all scattering shells.  $\Delta E_0$  is referenced to the inflection point of the absorption edge. The value of  $S_0^2$  was determined to be 0.66 by fitting the EXAFS spectrum of bulk Ru. The fit ranges are given by  $\Delta k$  and  $\Delta R$ .  $\Delta k$  is the range in  $k$ -space over which the spectrum can be fit and is determined by the quality of the data.  $\Delta R$  is the range in  $R$ -space over which the data is being fit;  $R_{max}$  and  $R_{min}$  are chosen at the points where the spectrum has a minimum at the end and beginning of the range of data being fit. The number of independent points,  $N_{ind}$ , is given by Stern's rule,  $N_{ind} = 2 + 2\Delta k\Delta R/\pi$  [22].

## 2.5. Adsorption experiments

Adsorption of  $H_2$ . Chemisorption experiments were carried out at  $25^\circ\text{C}$  using conventional Pyrex volumetric adsorption equipment [23]. The vacuum ( $10^{-6}$  mbar) was achieved with a liquid nitrogen-trapped mercury diffusion pump. The equilibrium pressure was measured with a Texas Instrument gauge (pressure range, 0–1000 mbar with an accuracy of 0.1 mbar). The catalyst sample was placed in a Pyrex cell and out-gassed at  $25^\circ\text{C}$  before applying a thermal treatment under vacuum at  $300^\circ\text{C}$  for 3 h (ramp of  $3^\circ\text{C}/\text{min}$  up to  $300^\circ\text{C}$ ), and then the chemisorption measurements were performed at  $25^\circ\text{C}$ . Reversible adsorption values are measured after out-gassing the samples at  $25^\circ\text{C}$  for 3 h. The oxidation/reduction cycles were performed in a reactor designed to avoid contact of the sample with the atmosphere. Typically, the sample was reduced under a  $H_2$  flow at  $300^\circ\text{C}$  during 3 h, followed by a desorption at  $300^\circ\text{C}$  for 3 h and an adsorption of  $H_2$  at  $25^\circ\text{C}$ . The H/Ru ratios are measured at  $25^\circ\text{C}$  under [0–250] mbar of  $H_2$ .

Adsorption of  $O_2$ . After desorption at  $300^\circ\text{C}$  for 3 h of silica supported particles, previously obtained by reaction under  $H_2$  at  $300^\circ\text{C}$ , adsorption of  $O_2$  was performed at  $25^\circ\text{C}$  and higher temperatures, and the O/Ru ratios are measured at  $25^\circ\text{C}$  under [0–250] mbar of  $O_2$ .

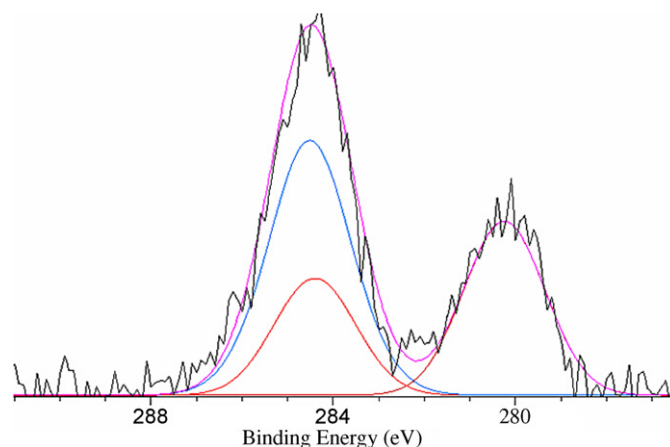


**Fig. 1.** XPS spectrum of  $[Ru_p/SiO_2]$  (purple) at the Ru3d level with the Ru3d (red) and C1s (blue) contributions. (For interpretation of the references to color in this figure legend, the reader is referred to the web version of this article.)

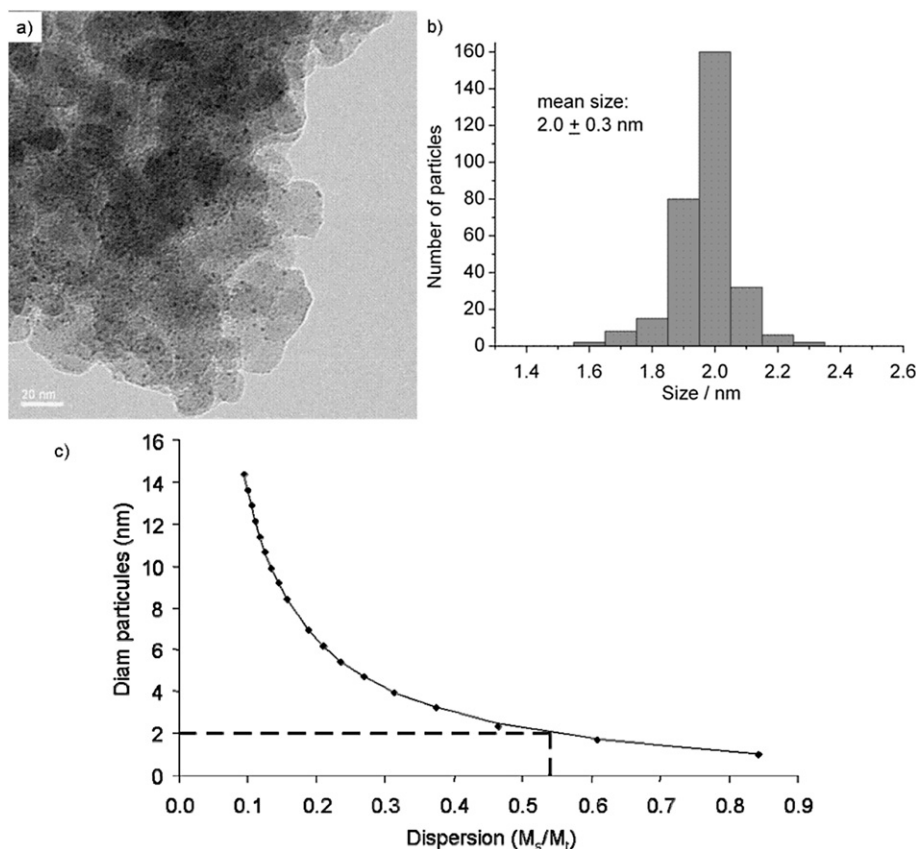


**Fig. 2.** Transmission electron microscopy of  $[\text{Ru}_p/\text{SiO}_2]$  (sample 2, 0.83 wt% Ru). (a) TEM image at a 20 nm scale. (b) Particle size distribution. (c) Determination of the dispersion using idealized hcp structure of ruthenium particles.

### 3. Results and discussion

#### 3.1. Characterization of $[\text{Ru}_p/\text{SiO}_2]$ by XPS

The XPS spectrum of  $\text{Ru}_p/\text{SiO}_2$  (sample 1) at the  $\text{Ru}3d$  level shows a binding energy of the  $\text{Ru}3d_{5/2}$  at 280.2 eV (Fig. 1), which is consistent with  $\text{Ru}^{(0)}$  [24]<sup>2</sup> of a totally reduced ruthenium sample, a crucial point for  $\text{H}_2$  adsorption measurements.

#### 3.2. Determination of the dispersion by transmission electron microscopy

The TEM images of  $[\text{Ru}_p/\text{SiO}_2]$  (sample 2), never exposed to air or  $\text{O}_2$ , show homogeneously dispersed particles (Fig. 2a) with a narrow particle size distribution centered at  $2.0 \pm 0.3$  nm (Fig. 2b). This is observed reproducibly with other  $[\text{Ru}_p/\text{SiO}_2]$  samples. Assuming that these particles adopt a hcp structure as for bulk Ru and small nanoparticles [25], the dispersion can be estimated to ca. 55% (Fig. 2c). Note that, when the samples are exposed to air (before introduction in the microscope as typically done in TEM analysis), the particles are difficult to observe. This is probably due to the formation of a  $\text{RuO}_2$  shell around the particles, which induces a loss of contrast. This could also explain the discrepancies between various reported data (*vide supra*).

#### 3.3. Calculation of the dispersion by EXAFS

The EXAFS spectrum of a  $[\text{Ru}_p/\text{SiO}_2]$  sample (Ru 0.9 wt%), its Fourier transform, and their corresponding fits are shown in Fig. 3.

Fitting the EXAFS data, using a model for Ru nanoparticles, gives a contribution of 10 neighbors in the first 2 shells (1.64–1.67 Å) (Table 1), which is consistent with nanoparticles having a mean size of  $2.3 \pm 0.7$  nm [26]. This result is fully consistent with what is observed by HR-TEM.

#### 3.4. Hydrogen and oxygen adsorption

First, the adsorption isotherms of  $\text{H}_2$  (total and reversible) can be calculated assuming a dissociative adsorption on the surface ruthenium atoms, following the Langmuir law, as described in Eq. (1), where  $Q_{\text{irr}}$  and  $Q_{\text{rev}}$  are respectively the amount of hydrogen irreversibly and reversibly adsorbed at room temperature,  $k$  is the reversible adsorption constant and  $P$  is the hydrogen pressure, note that  $Q_{\text{irr}}$  is not sensitive to  $P$ <sup>3</sup>

$$Q_{\text{ads}} = Q_{\text{irr}} + Q_{\text{rev}}(kP)^{1/2} / [1 + (kP)^{1/2}]. \quad (1)$$

The experimental and calculated values obtained for  $[\text{Ru}_p/\text{SiO}_2]$  are reported; in Fig. 4 (sample 2) and Table 2. The values of  $\text{H}/\text{Ru}_t$  correspond to extrapolation to infinite equilibrium pressure. Note that no measurable adsorption occurs on the support alone, and that adsorption of  $\text{H}_2$  on  $[\text{Ru}_p/\text{SiO}_2]$  reaches rapidly a plateau. These data, as well as the absence of effect of the Ru surface density ( $\text{mmol Ru nm}^{-2}$ ) on the  $\text{H}/\text{Ru}_s$  stoichiometry (*vide infra*), indicate that spill-over on the silica support does not contribute to a significant H adsorption. The silica supported ruthenium particles  $[\text{Ru}_p/\text{SiO}_2]$  adsorb 1.09  $\text{H}/\text{Ru}_t$  at equilibrium (sample 2, Ta-

<sup>2</sup> Note that the binding energies of  $\text{Si}2p$  and  $\text{O}1s$  are found at 103.6 and 532.9 eV respectively which are the exact values expected.

<sup>3</sup> The full adsorption models should be defined as  $Q_{\text{ads}} = Q_{\text{irr}}(k_{\text{irr}}P)^{1/2} / [1 + (k_{\text{irr}}P)^{1/2}] + Q_{\text{rev}}(k_{\text{rev}}P)^{1/2} / [1 + (k_{\text{rev}}P)^{1/2}]$ , but simplifies to  $Q_{\text{ads}} = Q_{\text{irr}} + Q_{\text{rev}}(kP)^{1/2} / [1 + (kP)^{1/2}]$ , because  $Q_{\text{irr}}(Q_{\text{irr}}(k_{\text{irr}}P)^{1/2}) / [1 + (k_{\text{irr}}P)^{1/2}]$  as the values obtained for  $k_{\text{irr}}$  are always  $\gg 1$  (ca. 1000).

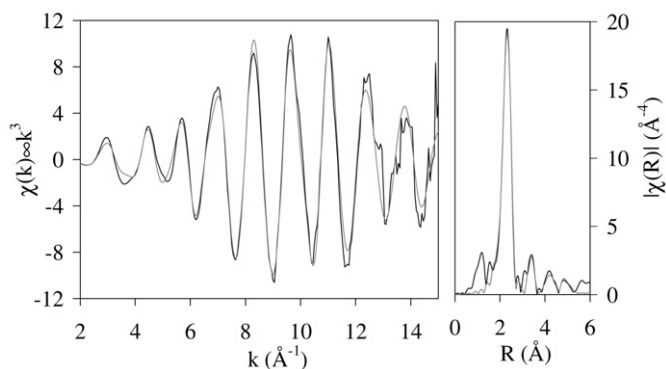


**Fig. 3.** EXAFS spectrum and Fourier transform of  $[\text{Ru}_p/\text{SiO}_2]$ . Data is black and fit is gray.

**Table 1**  
Fitted EXAFS parameters for  $[\text{Ru}_p/\text{SiO}_2]$ .<sup>a</sup>

Neighbor	Number of neighbors <sup>b</sup>	Distance (Å)	$\sigma^2$ (Å <sup>2</sup> )
Ru	4.9(3)	2.634(2)	0.0058(2)
Ru	4.9(3)	2.679(2) <sup>c</sup>	0.0058 <sup>c</sup>
Ru	4.5(4)	3.76(1)	0.008(1)
Ru	1.4(2)	4.4(1)	0.013(2)
Ru	12(2)	4.64(2)	0.0130 <sup>d</sup>
Ru	8(1)	5.06(7)	0.0130 <sup>d</sup>
Ru <sup>e</sup>	3.9(6)	5.30(3)	0.0130 <sup>d</sup>

Fit range:  $2 \text{ \AA}^{-1} < k < 15 \text{ \AA}^{-1}$ ;  $1.63 \text{ \AA} < R < 5.87 \text{ \AA}$ . Number of independent points: 37. Number of parameters: 11. R\_factor: 0.014.

<sup>a</sup>  $S_0^2 = 0.66$  (fixed, determined from fitting Ru foil),  $\Delta E_0 = -8(1) \text{ eV}$ ,  $R = 11(3) \text{ \AA}$ .

<sup>b</sup> Number of neighbors,  $N$ , determined using the formula for nanoparticles:  $N = N_0[1 - (3/4)(r/R) + (1/16)(r/R)^3]$ , where  $N_0$  is the coordination number for that shell in Ru metal (hcp structure),  $R$  is the radius of the particles, and  $r$  is the Ru–Ru distance of that set of atoms [26,27].

<sup>c</sup> The hcp structure of Ru contains two sets of 6 atoms, which have slightly different bond distances. Only change in bond distance and the Debye–Waller factor was used in fitting the first two shells.

<sup>d</sup> Debye–Waller factor same as for the fourth shell of atoms at 4.4 Å. Shell includes contributions from two multiple-scattering paths, which have the same parameters as the single scattering path.

<sup>e</sup> Shell includes contributions from two multiple-scattering paths, which have the same parameters as the single scattering path.

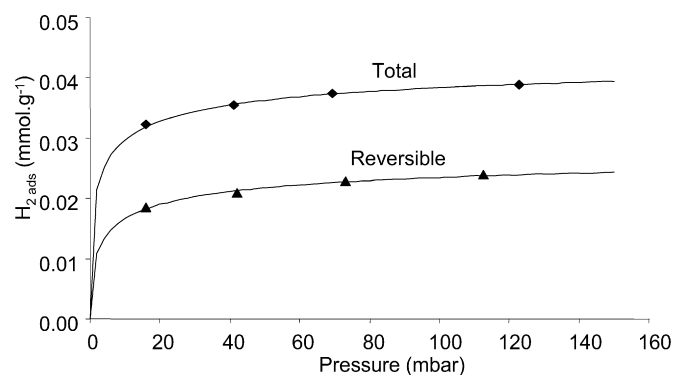


**Fig. 4.** Hydrogen adsorption on  $[\text{Ru}_p/\text{SiO}_2]$  (sample 2). (◆) Total adsorption. (▲) Reversible adsorption. (–) Simulated Langmuir adsorption isotherms.

**Table 2**  
 $\text{H}_2$  adsorption on  $[\text{Ru}_p/\text{SiO}_2]$ .

Sample	Ru (wt%)	$Q_{\text{irr}}(Q_{\text{rev}})$ (mmol g <sup>-1</sup> )	$k$ (mbar <sup>-1</sup> )	H/Ru <sub>t</sub>
$[\text{Ru}_p/\text{SiO}_2]$	0.66	0.0145 (0.017)	0.18	0.96
Sample 1	0.83	0.010 (0.029)	0.18	1.09
Sample 2	1.92	0.032 (0.072)	0.50	1.09

**Table 3**  
 $\text{O}_2$  adsorption on  $[\text{Ru}_p/\text{SiO}_2]$ .

Sample	Experimental value	
	O/Ru <sub>t</sub> (25 °C)	O/Ru <sub>t</sub> (200 °C)
$[\text{Ru}_p/\text{SiO}_2]$	1.40	–
Sample 2	1.44	–
$[\text{Ru}_p/\text{SiO}_2]$	–	1.87
Sample 3	–	–

**Table 4**  
 $\text{H}_2$  and  $\text{O}_2$  adsorption on  $[\text{Ru}_p/\text{SiO}_2]$  as a function of the number of oxidation/reduction cycles.

Cycle	Experimental values	
	H <sub>t</sub> /Ru	O/Ru (25 °C)
0	1.07	1.39
1	0.73	1.52
2	0.68	1.46
3	0.58	–

ble 2). Considering a dispersion of 55% (TEM), the stoichiometry is therefore 2.0 H/Ru<sub>s</sub>. In the case of isotherms of reversible  $\text{H}_2$ , the amount of H adsorbed on Ru is 0.70 H/Ru<sub>t</sub> which corresponds to 2/3 of the total amount. These H species correspond to more weakly adsorbed hydrogen on the surface, which are easily removed by evacuating the sample under vacuum at 25 °C.<sup>4</sup> Note that the value of 2H/Ru<sub>s</sub> is obtained reproducibly on a wide range of samples prepared at different loadings (0.66–1.92 wt%) using non-porous ( $[\text{Ru}_p/\text{SiO}_2]$ —samples 1–3) or mesoporous silica ( $[\text{Ru}_p/\text{SBA-15}]$ ).

Second, adsorptions of  $\text{O}_2$  have been performed (Table 3). At 25 °C, 1.4–1.5 O/Ru<sub>t</sub> were adsorbed irreversibly, and these values increased with time and temperature to reach the stable values of 1.9 O/Ru<sub>t</sub> after treatment at 200 °C for 2 h, which is in agreement with the formation of bulk RuO<sub>2</sub>.

Finally, the influence of oxidation/reduction cycles on  $\text{H}_2$  and  $\text{O}_2$  adsorptions has been studied (sample 2 of  $[\text{Ru}_p/\text{SiO}_2]$ , Table 4). Although the H/Ru<sub>t</sub> ratio decreases from 1.07 to 0.73 after the first oxidation/reduction cycle, the O/Ru<sub>t</sub> ratio (25 °C) remains almost constant (from 1.39 to 1.52). As further oxidation/reduction cycles are performed on this sample, the H/Ru<sub>t</sub> ratio slowly decreases while the O/Ru<sub>t</sub> ratio remains constant. This phenomenon is consistent with either the modification of adsorption properties of the particles upon oxidation/reduction cycles or most likely the increase of the metal particles dispersion.

#### 4. Conclusion

In conclusion, elemental analysis, XPS, EXAFS, TEM and adsorption measurements on  $[\text{Ru}_p/\text{SiO}_2]$  show that:

- 1) Fully reduced 2 nm size Ru nanoparticles supported on silica, free of strong ligands, such as CO or Cl<sup>-</sup>, and carbonous species, are obtained using a perhydrocarbyl complex as precursor.
- 2) Ru particles adsorb ca. 2H per surface ruthenium atoms (2H/Ru<sub>s</sub>) on various samples, so that this technique can be used to measure the dispersion of Ru particles.
- 3)  $\text{O}_2$  is an inappropriate probe for dispersion measurements because of partial oxidation of the bulk even at 25 °C, and the presence of irreversible process upon  $\text{H}_2/\text{O}_2$  cycles.

<sup>4</sup> The presence of 2 types of adsorbed hydrogen could be explained by either the presence of different adsorption sites (atop vs 3-fold sites, see for example Ref. [8b]) or an increase of the Ru–H bond strength with decreasing hydrogen coverage.



Finally, it is also worth pointing out that the H/M stoichiometry ( $2\text{H}/\text{Ru}_5$ ) is very close to this already obtained for Pt and Rh particles [4,6], and we are currently investigating the generality of this observation on other metal particles.

## Acknowledgments

R.B. and D.G. thank le Ministère de la Recherche et de l'Éducation and the Région Rhône-Alpes (Cluster 5) for graduate fellowships, respectively. We are all grateful to the CNRS (PICS program), CPE Lyon and IDECAT for financial supports. Portions of this work were performed at the LBNL, supported by the Director, Office of Science, Office of Basic Energy Sciences of the US Department of Energy under Contract No. DE-AC02-05CH11231, and at the Stanford Synchrotron Radiation Laboratory, a national user facility operated by Stanford University on behalf of the US Department of Energy, Office of Basic Energy Sciences.

## References

- [1] T. Bell Alexis, *Science* 299 (2003) 1688–1691.
- [2] M. Comotti, C. Della Pina, R. Matarrese, M. Rossi, *Angew. Chem. Int. Ed.* 43 (2004) 5812–5815; M. Frank, M. Baumer, *Phys. Chem. Chem. Phys.* 2 (2000) 3723–3737; C.R. Henry, *Appl. Surf. Sci.* 164 (2000) 252–259.
- [3] G.K. Borekov, A.P. Karnaukhov, *Zh. Fiz. Khim.* 26 (1952) 1814–1823; L. Spenadel, M. Boudart, *J. Phys. Chem.* 64 (1960) 204–207.
- [4] J.P. Candy, P. Fouilloux, A.J. Renouprez, *J. Chem. Soc. Faraday I* 76 (1980) 616–629.
- [5] C. Hubert, A. Frennet, *Catal. Today* 17 (1993) 469–482.
- [6] J.P. Candy, A. El Mansour, O.A. Ferretti, G. Mabilon, J.P. Bournonville, J.M. Basset, G. Martino, *J. Catal.* 112 (1988) 201–209.
- [7] H. Calvin, H. Bartholomew, *Roy. Soc. Chem.* 11 (1994) 93–126.
- [8] Note that the H/Ms stoichiometry could be dependant on the nature of the support, the particle shape, and other factors (presence of impurities...). This has recently been demonstrated in the case of platinum particles supported on zeolites, see for example: (a) Y. Ji, A.M.J. van der Eerden, V. Koot, P.J. Kooyman, J.D. Meeldijk, B.M. Weckhuysen, D.C. Koningsberger, *J. Catal.* 234 (2005) 376–384; (b) Y. Ji, V. Koot, A.M.J. van der Eerden, B.M. Weckhuysen, D.C. Koningsberger, D.E. Ramaker, *J. Catal.* 245 (2007) 415–427.
- [9] H. Kubicka, *J. Catal.* 12 (1968) 223–237.
- [10] R.A. Dalla Betta, *J. Catal.* 34 (1974) 57–60; R.A. Dalla Betta, *J. Phys. Chem.* 79 (1975) 2519–2525; R.A. Dalla Betta, M. Shelef, *J. Catal.* 48 (1977) 111–119; H.Y. Lin, Y.W. Chen, *Thermochim. Acta* 419 (2004) 283–290; J. Garcia-Anton, R. Axet, S. Jansat, K. Philippot, B. Chaudret, T. Pery, G. Buntkowsky, H.-H. Limbach, *Angew. Chem. Int. Ed.* 47 (2008) 1–6.
- [11] J.G. Goodwin Jr., *J. Catal.* 68 (1981) 227–232.
- [12] G. Lauth, E. Schwarz, K. Christmann, *J. Chem. Phys.* 91 (1989) 3729–3744.
- [13] S.Y. Chin, O.S. Alexeev, D. Amiridis, *Appl. Catal. A* 286 (2005) 157–166.
- [14] N.E. Buyanova, A.P. Karnaukhov, N.G. Koroleva, I.D. Ratner, O.N. Chernyavskaya, *Kinet. Katal.* 13 (1972) 1533–1539; K.C. Taylor, *J. Catal.* 38 (1975) 299–306; H. Kubicka, *React. Kinet. Catal. Lett.* 5 (1976) 223–228; H. Kubicka, B. Kuznicka, *React. Kinet. Catal. Lett.* 8 (1978) 131–136; G. Corro, R. Gomez, *React. Kinet. Catal. Lett.* 12 (1979) 145–150; P.G.J. Koopman, A.P.G. Kieboom, H. Van Bekkum, *J. Catal.* 69 (1981) 172–179.
- [15] D. Zhao, Q. Huo, J. Feng, B.F. Chmelka, G.D. Stucky, *J. Am. Chem. Soc.* 120 (1998) 6024–6036.
- [16] N. Kitajima, A. Kono, W. Ueda, Y. Morooka, T. Ikawa, *J. Chem. Soc. Chem. Commun.* (1986) 674–675.
- [17] P. Pertici, G. Vitulli, *Inorg. Synth.* 22 (1983) 176–181.
- [18] D.C. Koningsberger, *R. Prins, X-Ray Absorption: Principles, Applications, Techniques of EXAFS, SEXAFS, and XANES*, Wiley, New York, 1988.
- [19] B. Ravel, M. Newville, *Phys. Scr.* T115 (2005) 1007–1010.
- [20] M. Newville, *J. Synchrotron Rad.* 8 (2001) 322–324.
- [21] J.J. Rehr, R.C. Albers, S.I. Zabinsky, *Phys. Rev. Lett.* 69 (1992) 3397–3400.
- [22] E.A. Stern, *Phys. Rev. B* 48 (1993) 9825–9827.
- [23] J.P. Candy, A.E. Mansour, O.A. Ferretti, G. Mabilon, J.P. Bournonville, J.M. Basset, G. Martino, *J. Catal.* 112 (1988) 201–209.
- [24] N. Chakroune, G. Viau, S. Ammar, L. Poul, D. Veautier, M.M. Chehimi, C. Mangeney, F. Villain, F. Fievet, *Langmuir* 21 (2005) 6788–6796; V. Mazzieri, F. Coloma-Pascual, A. Arcoya, P.C. L'Argentiere, N.S. Figoli, *Appl. Surf. Sci.* 210 (2003) 222–230; K.W. Park, J.-H. Choi, B.-K. Kwon, S.-A. Lee, Y.-E. Sung, H.-Y. Ha, S.-A. Hong, H. Kim, A. Wieckoski, *J. Phys. Chem. B* 106 (2002) 1869; C.D. Wagner, W.M. Riggs, L.E. Davis, F.J. Moulder, G.E. Muilenberg, in: *Physical Electronics Division*, vol. 55, Perkin-Elmer, Eden Prairie, MN, 1979, p. 344.
- [25] K. Pelzer, O. Vidoni, K. Philippot, B. Chaudret, V. Collière, *Adv. Funct. Mater.* 13 (2003) 118–126; K. Pelzer, B. Laleu, F. Lefebvre, K. Philippot, B. Chaudret, J.P. Candy, J.M. Basset, *Chem. Mat.* 16 (2004) 4937–4941; D. Wostek-Wojciechowska, J.K. Jeszka, C. Amiens, B. Chaudret, P. Lecante, *J. Colloid Interface Sci.* 287 (2005) 107–113.
- [26] S. Calvin, S.X. Luo, C. Caragianis-Broadbridge, J.K. McGuinness, E. Anderson, A. Lehman, K.H. Wee, S.A. Morrison, L.K. Kurihara, *Appl. Phys. Lett.* 87 (2005) 233101–233103.
- [27] S. Calvin, C.J. Riedel, E.E. Carpenter, S.A. Morrison, R.M. Stroud, V.G. Harris, *Phys. Scr.* T115 (2005) 744–748.